Chemical Engineering Journal 165 (2010) 563–572

Contents lists available at ScienceDirect

Chemical Engineering Journal

journal homepage: www.elsevier.com/locate/cej

An environmentally friendly batch bioadsorption study of the radionuclides ^{67}Ga from aqueous solutions by fibrous tea waste

Hayrettin Eroglu[a,*], Erhan Varoglu[a], Sinan Yapıcı[b], Ali Sahın[a]

[a] Atatürk Üniversitesi, Araştırma Hastanesi, Nükleer Tıp Ana Bilim Dalı, 25240 Erzurum, Turkey
[b] Atatürk Üniversitesi, Mühendislik Fakültesi, Kimya Mühendisliği Bölümü, 25240 Ezurum, Turkey

ARTICLE INFO

Article history:
Received 20 July 2010
Received in revised form
28 September 2010
Accepted 29 September 2010

Keywords:
Bioadsorption
Kinetics
Radiation
Radionuclides
Gallium

ABSTRACT

The radionuclides ^{67}Ga is used in nuclear medicine. This paper presents a bioadsorption study of ^{67}Ga from aqueous solution by solid tea factory waste. The experimental parameters were chosen as temperature, pH, stirring speed, nominal particle size and bioadsorbent dose in the ranges of 10.0–40.0 °C, 2.0–8.0, 300–720 rpm, 0.15–1.4 mm and 1.0–15.0 g/L, respectively. The most effective parameter was determined to be pH, and then temperature, particle size, and bioadsorbent dose in decreasing order. Fourier transform infrared spectroscopy was performed for the characterisation of the bioadsorption of ^{67}Ga on tea waste. The equilibrium results showed that the data exhibited good agreement with the isotherm models of Freundlich, Halsey, and Handerson and Smith. In thermodynamic analysis, ΔG and ΔH values were determined and their values demonstrated that the bioadsorption process was endothermic and spontaneous. Bioadsorption kinetics analysis proved that the rate corresponded to a pseudo second order model, and that the bioadsorption mechanism is governed by intra-particular diffusion.

1. Introduction

Nuclear medicine frequently utilizes radionuclides for medical diagnosis and therapy for some illnesses. However, the radiations such as X and gamma rays, alpha, beta particles, neutrons and auger electrons cause changes in molecular level in the cells through which they passed, by activating molecules and atoms in the cell. Ionized radioactive species can also cause molecular, chemical and physical changes in living cell, which can be curable or non-curable depending on the intensity, period, and kind of the subjected radiation. Consequently, radiation can oppress the growth of living cells, cause giant cell formation, result in breakage, adhesion or bending of chromosomes, and cause the death of cells. Radiation can have catastrophic effects on hematopoetic, reproductive, gastrointestinal, neural network systems, in addition to the skin and eyes, and other elements of body systems such as the heart, kidney, liver and pancreas, etc [1].

One of radionuclides used frequently in nuclear medicine is gallium citrate. Decay of radionuclides ^{67}Ga yields ^{67}Zn and gamma rays as shown in the following radioactive reaction. The half-life of the decay reaction is 78.25 h [2].

$$^{67}\mathrm{Ga} \rightarrow {}^{67}\mathrm{Zn} \quad +\gamma^{-2}.\ 93\,\mathrm{KeV}(\%38) + \gamma^{-3}.\ 185\,\mathrm{KeV}(\%24) \\ +\gamma^{-5}.\ 300\,\mathrm{KeV}(\%16) + \gamma^{-6}.\ 394\,\mathrm{KeV} \qquad (1)$$

After visualization or therapy using the radionuclide, the harmful aqueous wastes are produced from the excrement of the patients and by unused radioactive chemicals. The discharged radionuclides can cause severe damage, and their biological effects can be very serious. Due to the serious and fatal effects of the radiation, the observance of the of protection methods such as keeping some distance, shielding, and leaving to time is very important. Therefore, the treatment of the aqueous waste from nuclear medicine centers to the environment is very important and a legal obligation, before discharging to the environment [3].

The precaution for reducing this problem is to retain liquid wastes in lead tanks and solid wastes in lead chambers until the radioactivity level decays to a certain value before discharging into the environment. However, this method is expensive, cumbersome and impractical for avoiding the harmful effects of radioactivity. Finally, diluted radionuclides are discharged to the environment before their activity is reduced to a harmless level. In addition to the contamination due to radioactivity, radionuclides can also cause heavy metal contamination because they are converted to stable metal ions in their stable state. When they mix with underground water, their harmful effects become unavoidable [1]. Therefore, the removal of these ionised radioactive substances from liquid wastes is of vital importance.

Various methods exist for removing ionised species from waste water, such as reverse osmosis, ion-exchange, precipitation and coagulation. However, these physicochemical methods are quite expensive and are not so effective in removing radionuclides when they exist in aqueous waste in low concentrations. Therefore, after

* Corresponding author. Tel.: +90 442 231 6653; fax: +90 442 231 2766.
E-mail address: heroglu@atauni.edu.tr (H. Eroglu).

1385-8947/$ – see front matter © 2010 Elsevier B.V. All rights reserved.
doi:10.1016/j.cej.2010.09.074

Nomenclature

C	concentration of adsorbate in the solution at equilibrium ($mg\,L^{-1}$)
D	diffusion coefficient (cm^2/s)
E	bioadsorption free energy ($J\,mol^{-1}$)
E_A	activation energy ($J\,mol^{-1}$)
G	Gibbs free energy ($J\,mol^{-1}$)
H	enthalpy ($J\,mol^{-1}$)
h	the initial bioadsorption rate
K	constant related to bioadsorption capacity ($L\,g^{-1}$)
k	kinetic rate constant
k_D	the distribution coefficient
K_1	constant related to bioadsorption energy ($mol^2\,kJ^{-2}$)
k_i	the intraparticular diffusion coefficient ($mg/g.s^{0.5}$)
n	constant related to bioadsorption intensity
q	adsorbed amount per amount adsorbent at equilibrium ($mg\,g^{-1}$)
r	the radius of the adsorbent particle (cm)
R	ideal gas constant ($8314\,J\,K^{-1}\,mol^{-1}$)
R	regression coefficient
S	entropy ($J\,mol^{-1}\,K^{-1}$)
T	absolute temperature (K)
t	time (min)
W and W_b	constant parameters for the Smith model

Subscript

1/2	half-life times
ads	adsorbed
e	equilibrium
s	the theoretical monolayer saturation capacity ($mg\,g^{-1}$)
o	initial value
t	any time
thr	theoretical

Greek letters

Δ	change
α	Elovich coefficient (the initial sorption rate ($mg\,g^{-1}\,min^{-1}$))
β	Elovich coefficient (desorption constant ($g\,mg^{-1}$))
ε	Polany potential
μ	micro

the treatment of the radioactive aqueous waste using physico-chemical methods, the waste still contains radionuclides. As an alternative, the use of bioadsorbents for removing radionuclides has some advantages over other methods and is becoming more important [4,5]. Many microorganisms, such as funguses, yeasts, bacteria, and marine organisms, can adsorb anionic and cationic substances from aqueous media [6–10]. In this context, I-131 used in nuclear medical applications was removed from aqueous solution by using Amberlite which is an ion-exchanger [11]. Koshima used the resins Amberlite-XAD and Chelex100 to remove metal ions from aqueous HCl solutions [12]. Osmanlioglu studied the adsorption of radionuclides (^{137}Cs, ^{60}Co, ^{90}Sr and ^{110m}Ag) on zeolites, and Clinoptilolite were shown to have a high selectivity for ^{137}Cs and ^{110m}Ag as sorbent [13]. Activated carbon has also been used to remove some radioactive ions from aqueous solutions, for example, uranium by Kütahyalı [14] and iodine by Sinha et al. [15].

In Turkey, the upper limit for ^{67}Ga in liquid waste is determined to be 1 μCi by related regulations [3]. Weekly gallium consumption in nuclear medical centers in Turkey is between 8000 and 24,000 μCi of ^{67}Ga. For this purpose, the waste is kept in lead tanks for a period of 10 times longer than the half-life period of radionuclides [16]. Therefore, the liquid waste consisting of urine and the waste water from showers of patients, etc., must be kept in lead tanks for quite a long time, minimum 1 month, before discharging to the environment. This is a very cumbersome and expensive method for disposing of the radioactiwe waste. These wastes occupy large areas at the site of operation, creating some environmental, operational and economical problems. In the eastern Black Sea Region of Turkey, The tea factories owned by the government produce approximately 20 thousand tones of solid tea waste each year. When the waste generated by private tea factories is added to this number, the total amount of waste generated increases to more than 30 thousand tones [17]. Little is done to use these solid wastes. Therefore, the aim of the present work is to use the biological solid waste of a tea factory as a bioadsorbent to remove radionuclides ^{67}Ga from aqueous media.

Table 1
Some properties of fibreous tea waste.

Density (g/cm^3)	0.119
Particle size (mm)	0.212–0.150
BET surface area (m^2/g)	0.702
Zeta potential of FTW at pH 2.0 (mV)	−40

2. Materials and methods

2.1. Bioadsorbent

The solid tea waste was provided by the Cumhuriyet tea plant in Rize in the eastern region of the Black Sea. Specifications for fibrous tea waste (FTW) derived from the under-chimney of the factory are given in Table 1. Before using FTW, it was first washed by distilled water several times until it yielded colourless filtered water. Subsequently, it was dried at room temperature. The dried FTW was ground and sieved to obtain selected nominal particle size fractions.

As seen in Fig. 1, bioadsorbent consisted of mainly carbon and oxygen in the ratios of, 57.458% and 37.281%, respectively. In addition, it contains the metals such as Se, Zn, Cu, Ni, Fe, Mn.

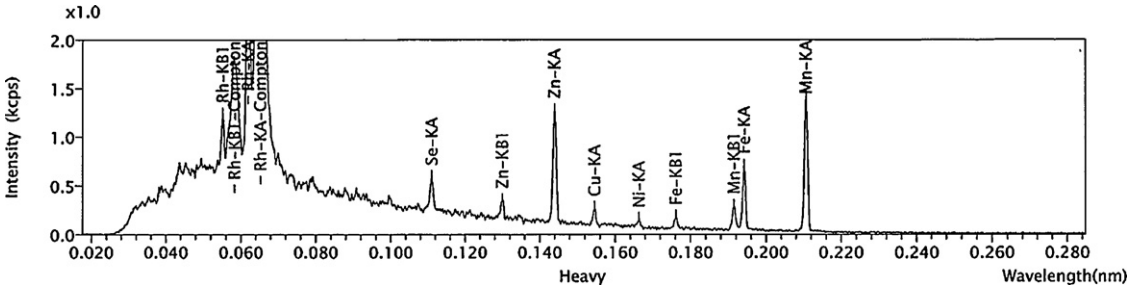

Fig. 1. XRF spectra of FTW.

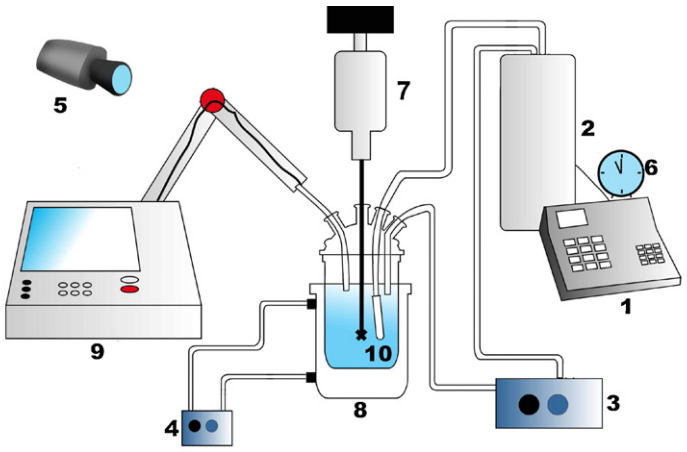

1. Radioactivity dosimeter	4. Circulating bath	7. Mechanical stirrer
2. Radioactivity reading chamber	5. Video camera	8. Jacketed adsorption vessel
3. Pump	6. Clock	9. pH meter
		10. Fitler

Fig. 2. The experimental set up for bioadsorption process [18].

2.2. Experimental system

The batch bioadsorption system used in the present research is shown in Fig. 2. In this experimental system, all safety precautions were implemented such that the operator was exposed to radioactivity at the minimum level possible. A little fraction of the solution in the vessel was circulated continuously through the radioactive dosimeter to measure the bioadsorbtion with time. The details of this experimental system are given in Ref. [18].

The temperature, initial pH, bioadsorbent dose, stirring speed and nominal particle size were selected as experimental parameters. While the effect of one of these parameters was investigated, the values of the other parameters were kept constant at 2.0 for the initial pH, 10 g/L for bioadsorbent dose, 600 rpm for stirring speed, 0.150–0.212 mm for particle size, and 20 °C for temperature.

Soma preliminary experiments with no bioadsorbent particle in the medium showed that no bioadsorbtion took place by the solid surfaces of the system, such as the vessel, the filter, the tubes.

2.3. Preparation of the radioactive solution

The ^{67}Ga solution was prepared by considering the production date. A certain amount of this solution was added into the bioadsorption vessel, whose temperature, stirring speed, bioadsorbent dose and initial pH value were previously set and the particles with a given nominal size is added, to obtain a 500 mL-solution with an initial radionuclide concentration of approximately 500 μCi. This concentration was selected because it approximates the radioactivity level of the liquid waste produced by nuclear medicine.

2.4. Fourier transform infrared spectroscopy (FTIR)

FTIR studies were performed for the characterisation of the bioadsorption mechanism of ^{67}Ga on FTW. The FTIR spectra were obtained and transferred to Microsoft Excel using a Perkin–Elmer Spectrum One Model FTIR spectrometer.

3. Results and discussion

The bioadsorption experiments of ^{67}Ga on FTW demonstrated that the equilibrium was reached in approximately 120 min; therefore, the bioadsorption values at 120 min were used for the calculations. The effects of the parameters on bioadsorption were determined and the results are illustrated in plots in Fig. 3.

3.1. Effect of pH

For observation of the effects of pH on the bioadsorption of ^{67}Ga with FTW, initial pH values of 2.0, 4.0, 6.0, 7.0, and 8.0 were tested. No considerable change in the initial pH was observed during the bioadsorption process. Therefore, the initial pH was taken as the equilibrium pH value. The change in the bioadsorption yield with pH is illustrated in Fig. 3(a). The change in the bioadsorption yield did not exhibit a regular behaviour with the change in the initial pH value. The greatest removal of ^{67}Ga was obtained at pH value of 2 followed by pH 4. The bioadsorption yield values at pH 2 were nearly the same as the values at pH 4, while the removal yields were lower at the initial pH values of 6.0, 7.0 and 8.0. The removal percentages of ^{67}Ga in 120 min, which are the equilibrium values, were 77.4% at pH 2 and 70.4% at pH 4. For the other pH values, the equilibrium removal percentages remained below approximately 40%.

Ga^{+3} ions are rapidly hydrolysed in aqueous medium yielding different chemical compounds depending upon the pH of the medium, as shown in Eqs. (2)–(5):

$$[Ga]^{+3} + H_2O = [Ga(OH)]^{+2} + H^+, \quad (2)$$

$$[Ga(OH)]^{+2} + H_2O = [Ga(OH)_2]^{+} + H^+, \quad (3)$$

$$[Ga(OH)_2]^{+} + H_2O = [Ga(OH)_3] + H^+, \quad (4)$$

$$[Ga(OH)_3] + H_2O = [Ga(OH)_4]^{-} + H^+, \quad (5)$$

To avoid the hydrolysis of the gallium ions in physiologic media, gallium in the form of gallium citrate is used as a radiopharmaceutical in nuclear medicine applications. Fig. 4 illustrates the formation of gallium chemicals in aqueous medium at different pH values. Gallium exists primarily as free gallium ions at approximately pH 2. As the pH increases, the gallium ions convert to $Ga(OH)_3$ and $[Ga(OH)_4]^-$. The zeta potential value of the bioadsorbent was −40 mV at pH 2. Therefore, at this pH value, the bioadsorption can be mainly driven by attraction of the free $[Ga]^{+3}$ ions with a positive charge toward the bioadsorbent surface having a negative

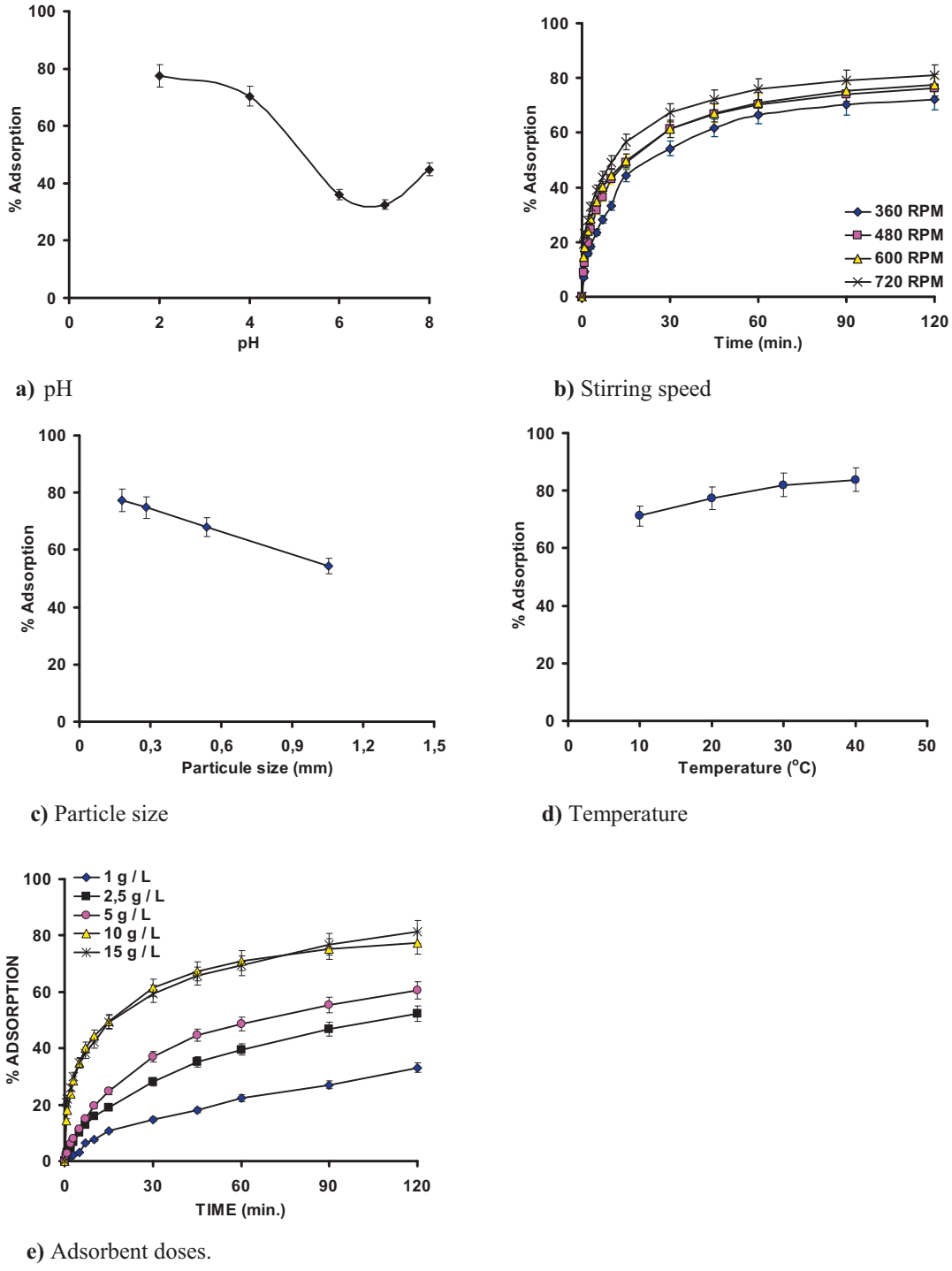

Fig. 3. Effect of experimental parameters on bioadsorption.

electrical charge [19]. At higher pH values, gallium forms gallium hydroxide or other ligands, of which the first one is neutral and the others are negatively charged compounds. Therefore, as the pH increases bioadsorption decreases due to the depletion effect of repulsion between the negative charges of gallium ligands and the bioadsorbent surface. Consequently, this behavior indicated that the process was mainly occurred due to physical attraction [20]; that is, it can be said that the electrostatic forces can have an important effect on the bioadsorption of Ga due to the interaction between positively charged Ga ions and oppositely charged bioadsorbent surface.

3.2. Effect of stirring speed

The effect of the stirring speed on the bioadsorption process was evaluated at the values of 360, 480, 600 and 720 rpm. The plot of the bioadsorption percentage versus the bioadsorption period is presented in Fig. 3(b) for different values of the stirring speed. No emphasized effect of the stirring speed was observed; however, the plot illustrates that the bioadsorption percentage increased slightly as the stirring speed increased. At equilibrium, the bioadsorption yield was 80.9% at 720 rpm, and the yield decreased to 74.3% when the stirring speed was reduced to 320 rpm. This small change can

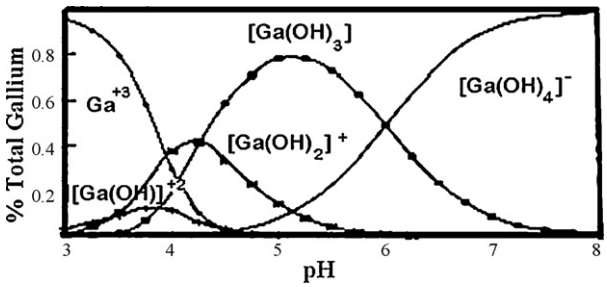

Fig. 4. Change of chemical structure of gallium hydroxide with pH [19].

be attributed to the thinning of the liquid film around the bioadsorbent particle with increased stirring speed which results in a slight increase in the rate of transfer of ^{67}Ga components to the surface of the bioadsorbent. This behaviour can also be an indication that the bioadsorption process is not controlled by mass transfer of ^{67}Ga through the liquid film layer surrounding the particle.

3.3. Effect of bioadsorbent particle size

To determine the effect of the bioadsorbent nominal particle size on the bioadsorption process, the particle sizes of 1.40–0.710, 0.710–0.355, 0.355–0.212, and 0.212–0.150 mm were examined. The experimental results are presented in Fig. 3(c) in a plot of the bioadsorption percentage versus time for different particle size values. The figure shows that the change in particle size has a considerable effect on the bioadsorption process. The degree of bioadsorption increased as the particle size decreased; for example, at equilibrium, 77.4% of the initial activity of ^{67}Ga was removed at a particle size of 0.150–0.212 mm, whereas the yield was reduced to 54.3% when a larger nominal particle size of 0.710–1.400 mm was used. This can be explained by the increase in the outer surface area per mass of the solid and the decrease in the nominal transfer distance through the pores in the particle as the particle size decreases. The pronounced effect due to particle size demonstrated that the diffusion of ^{67}Ga through the diffusion through the pores in the bioadsorbent may be an important step in controlling the rate of the bioadsorption process.

3.4. Effect of temperature

To determine the effect of temperature on the bioadsorption process, the bioadsorption process was carried out at different temperatures of 10, 20, 30 and 40 °C. The effect of the temperature on the bioadsorption process as a function of bioadsorption period is illustrated in Fig. 3(d). This figure shows that as the temperature rises the bioadsorption percentage increases. The highest percentage of the removal was obtained at 40 °C; for a bioadsorption period of 120 min, approximately 83.8% of the initial activity of ^{67}Ga was adsorbed at 40 °C while the bioadsorption yield reduced to 71.2% at 10 °C. The effect of temperature on the process is slightly greater than that of stirring speed and less than the effects of pH and particle size. The increase of the yield with temperature can be an indication that the bioadsorption is an endothermic chemical process.

3.5. Effect of bioadsorbent dose

For the study of the effect of the bioadsorbent dose on the bioadsorption, the experiments were conducted at the bioadsorbent dose values of 1.0, 2.5, 5.0, 10.0 and 15.0 g solid/L while the values of the remaining parameters was held constant at a pH of 2.0, a particle size of 0.150–0.212 mm, a stirring speed of 600 rpm, and a temperature of 20 °C. The effect of the bioadsorbent dose on the bioadsorption is illustrated in Fig. 3(e) as a function of the bioadsorption period. As the bioadsorbent dose increased, the bioadsorption percentage increased. The greatest removal percentage was obtained at 15 g/L for an bioadsorption period of 120 min; approximately 81.2% of the initial activity of ^{67}Ga was adsorbed at 15 g/L while the bioadsorption yield decreased to 33.1% at 1 g/L. The increase of the bioadsorption as the bioadsorbent dose increased resulted from the increase of the available bioadsorption area at a constant initial value of ^{67}Ga concentration.

3.6. Bioadsorption isotherms

The graphical representation between the adsorbed amount per amount of adsorbent, q, and non-adsorbed amount per amount of solution, c, at constant temperature is referred to as the bioadsorption isotherm. Numerous attempts have been made to derive mathematical expressions to fit measured bioadsorption isotherms. However, no single bioadsorption isotherm equation has been suggested to explain bioadsorption data. Therefore, various isotherm models exist depending upon bioadsorption mechanisms.

In the present study, the equilibrium was changed by using different amounts of the bioadsorbent instead of changing the initial concentration of ^{67}Ga because increasing the concentration of the radioactive species is a safety factor due to higher levels of radioactivity. The isotherm models for the bioadsorption process were studied by using the data given in Fig. 3(e). The models yielding meaningful results are discussed in the following text.

Statistical analysis demonstrated that the isotherm data for this research fitted well to the isotherm models of Freundlich, Halsey, Henderson and Smith, which were developed for the multi-layered bioadsorption process, and did not fit to the Langmuir model.

The fit of the data to the Freundlich, Halsey, Henderson and Smith isotherms is an indication that the active sites on the bioadsorbent surface had heterogeneous structure which consisted of the bioadsorption sites of various species and that the bioadsorption is multilayered [18,20–24]. The model equations, the values of the constants derived from these equations and the square of the correlation coefficients of the above models are presented in Table 2. The Langmuir isotherm model was also tested, but it was found that the data did not fir well to this model. However, the observation that the data do not agree with the Langmuir model is meaningful because this model is used to explain single-layered bioadsorption.

These isotherms are commonly used to represent physical bioadsorption processes. However, if the effect of temperature on bioadsorption is also considered, it can be concluded that, the process is not singly a physical or chemical process; that is, a combined physicochemical process is likely [25].

3.7. Thermodynamic analysis

The thermodynamic parameters of the Gibbs free energy change (ΔG), the enthalpy change (ΔH) and the entropy change (ΔS) were determined to evaluate the thermodynamic character of the bioadsorption process. The Gibbs free energy change of the process is related to the distribution constant (k_D) as follow [18]:

$$k_D = \frac{C_{ads}}{C_{non-ads}} \tag{10}$$

$$\Delta G = -RT \ln k_D \tag{11}$$

The Gibbs free energy change (ΔG) is related to the enthalpy and entropy change as follow:

$$\Delta G = \Delta H - T\Delta S \tag{12}$$

Table 2
Model constants and correlation coefficients of isotherm models.

Adsorption isotherm	Model equation		Value	R^2
Freundlich	$q = KC^{1/n}$	(6)	$n = 0.739$ $K = 13.72$	0.969
Halsey	$\ln q = [(1/n)\ln K] - (1/n)\ln[\ln(1/C)]$	(7)	$n = 0.071$ $K = 4.564$	0.972
Henderson	$\ln q = (1/n)\ln[-\ln(1-C)] - (1/n)\ln K$	(8)	$n = 0.739$ $K = 0.145$	0.970
Smith	$q = W_b - W\ln(1-C)$	(9)	$W = 0.560$ $W_b = -6 \times 10^{-6}$	0.952

Table 3
Thermodynamic parameters of the gallium ions adsorption on the tea waste at different temperatures.

Temperature (K)	ΔG (J mol^{-1})	ΔH (J mol^{-1})	ΔS (J mol^{-1})
283	−2135.1	18422	728
293	−3006.3		
303	−3829.1		
313	−4286.6		

The values of ΔG for different temperature values, calculated by using Eqs. (10) and (11), are given in Table 3. The plot of ΔG versus T yielded a straight line as shown in Fig. 5. The values of ΔH and ΔS can be obtained from the intercept and the slope of the line, respectively. The values of ΔH and ΔS were calculated to be equal to 18,422 J mol^{-1} and 728 J mol^{-1} K^{-1}, respectively.

Gibbs free energy change (ΔG) values were found to be increasingly negative as temperature increased which indicated the feasibility and spontaneity of the bioadsorption process of gallium on fibrous tea waste. The value for the enthalpy change (ΔH) calculated for ^{67}Ga was determined to be positive, which indicated the endothermic nature of bioadsorption process. The positive entropy change (ΔS) for the present case can be attributed to the increase in the number of species and, hence, the randomness in the (solid + liquid) interface due to the release of water molecules and hydroxyl ions from ^{67}Ga when the adsorbate species become adsorbed. For this bioadsorption process, a ΔH value less than 40 kJ mol^{-1} indicates that the bioadsorption of ^{67}Ga by fibrous tea waste has also a physical character besides its chemical side [26].

3.8. Evaluation of bioadsorption energy

The Dubinin–Radushkevich (D–R) equation was chosen for evaluating the bioadsorption energy. This relationship is expressed mathematically in Eqs. (13)–(15):

$$\ln q = \ln q_s - K_1\varepsilon^2 \quad (13)$$

$$\varepsilon = RT\ln(1 + 1/C) \quad (14)$$

$$E = \frac{1}{\sqrt{2K_1}} \quad (15)$$

The value of E [27] which is defined as the free energy change when one mole of ions transfers from the solution to the solid surface—is calculated using the value of K_1 [26]. The plot for this data is presented in Fig. 6. From Eqs. (13)–(15), it was determined that $K_1 = 1 \times 10^{-8}$, $q_s = 0.013$, and $E = 7071.1$ J mol^{-1}. The value of the square of the correlation coefficient, $R^2 = 0.966$, shows that $\ln q$ is a strong function of ε^2.

In the D–R equations, the E value provides information about whether bioadsorption mechanisms involve chemical ion-exchange or physical bioadsorption. Because the values of E were smaller than 8000 J mol^{-1}, the bioadsorption of ^{67}Ga on fibrous tea waste was indicated to result from physical bioadsorption [28]. However, although lower values of activation energy and bioadsorption energy could be an indication that the process has primarily physical character, the fact that the bioadsorption yield increases with increasing temperature shows that the process also has physico-chemical character.

3.9. FTIR spectroscopy

FTIR spectroscopy is commonly used in organic chemistry. This technique provides a tool for determining the functional groups in an organic molecule. In order to determine the primary functional groups of the TW employed in ^{67}Ga bioadsorption, FTIR spectra were obtained before and after bioadsorption (Fig. 7). The decreasing signal of functional groups in the spectrum was interpreted to indicate that these groups participated in the bioadsorption process. As seen in Table 4, the FTIR spectra illustrate that FTW

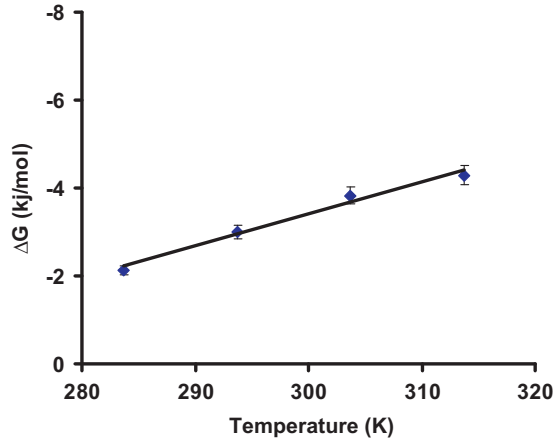

Fig. 5. Plot of ΔG versus T.

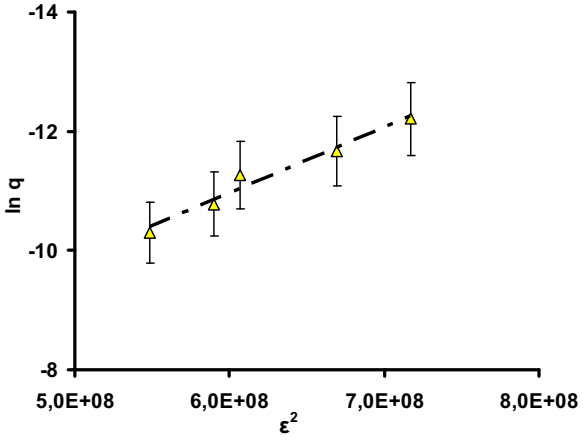

Fig. 6. Fit of data to D–R equation.

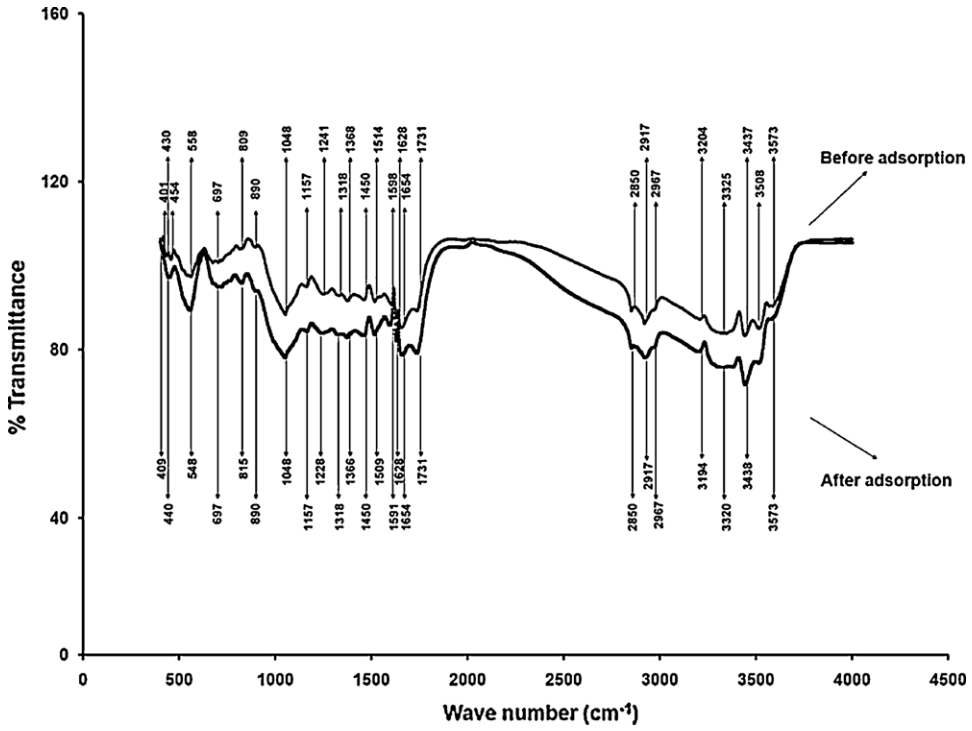

Fig. 7. IR spectrum of FTW.

is represented by 26 bioadsorption bands. The spectral analysis, before and after ^{67}Ga bioadsorption, indicated that, among the 26 bioadsorption bands, nine significant band decreases of the functional groups on the bioadsorbent were detected at 3325, 3204, 1598, 1514, 1241, 558, 454, 430, and 401 cm^{-1}. These bands were involved in ^{67}Ga bioadsorption. The groups affected by the bioadsorption of ^{67}Ga include –OH, N–H (stretching), secondary amines, –SO_3 (stretching), –C–C–, and amine groups [29–34]. These various functional groups can form complexes by combining with gallium; 77.4% of the initial activity of ^{67}Ga in the solution was adsorbed by the fibrous tea waste at pH 2 in 120 min. The bioadsorption process was demonstrated to occur quite rapidly. Significant reduction in 9 out of 26 bands can indicate that the bioadsorption process occurs partly chemically by interaction with some of these active groups.

3.10. Bioadsorption kinetics

Kinetic models for the bioadsorption process are related to the removal rate of the adsorbate from the solution. A bioadsorp-

Table 4
FTIR spectrum of FTW before and after bioadsorption.

IR Peak	Frequency (cm^{-1})			Group
	Before ads.	After ads.	Differences	
1	3573	3577	+4	Bonded hydroxil (−OH) gruoups
2	3508	3507	−1	Bonded hydroxil (−OH) gruoups
3	3437	3438	+1	Bonded hydroxil (−OH) gruoups
4	3325	3320	−5	Bonded hydroxil (−OH) gruoups
5	3204	3194	−10	N–H stretching
6	2967	2967	0	Aliphatic
7	2917	2917	0	Aliphatic C–H groups
8	2850	2850	0	Aliphatic C–H groups
9	1731	1731	0	C═O stretching
10	1654	1654	0	C═O stretching
11	1628	1628	0	C═O stretching
12	1598	1591	−7	Seconder amine gruops
13	1514	1509	−5	Seconder amine groups
14	1450	1450	0	Symmetric bending of CH_3
15	1368	1366	−2	Symmetric bending of CH_3
16	1318	1318	0	Symmetric bending of CH_3
17	1241	1228	−13	–SO_3 stretching
18	1157	1157	0	C–O stretching of ether groups
19	1048	1048	0	C–O stretching of ether groups
20	890	890	0	Aromatic –CH stretching
21	809	818	+9	Aromatic –CH stretching
22	697	712	+15	–CN stretching
23	558	547	−11	–C–C–groups
24	454	440	−14	Amine groups
25	430	409	−21	Amine groups
26	401	Unappeared	–	Amine groups

Table 5
Kinetic equations used for analysis of kinetic data.

Kinetic equation	Linear form of equation		Plot	Reference
Pseudo-first order	$\ln(q_e - q_t) = \ln q_e - kt$	(16)	$\ln(q_e - q_t)$ versus t	[31–33]
Pseudo-second order	$(t/q_t) = 1/(kq_e{}^2) + (1/q_e)t$	(17)	t/q_t versus t	[31–33]
	$h = kq_e^2$	(18)		
Elovich	$q_t = (1/\beta)\ln(\alpha\beta) + (1/\beta)\ln t$	(19)	q_t versus $\ln t$	[31–33]

Table 6
Kinetic parameters for the removal of ^{67}Ga by FTW.

Kinetic models		Pseudo- first order kinetic models			Pseudo-second order kinetic model				Elovich equation		
Parameters		R^2	K	$q_{e,teo} \times 10^6$	R^{2*}	k	$h \times 10^6$	$q_{e,teo} \times 10^6$	R^2	$\beta \times 10^{-6}$	$\alpha \times 10^8$
Temp. (°C)	10	0.992	0.028	6.485	0.977	16266.4	1	7.841	0.936	1	0.674
	20	0.982	0.037	6.187	0.995	20732.6	1.597	8.778	0.987	1	1.832
	30	0.912	0.033	5.142	0.997	28597.2	2.013	8.390	0.986	1	4.979
	40	0.862	0.028	4.231	0.997	41318.1	2.870	8.335	0.992	1	54.88
pH	2	0.982	0.037	6.187	0.995	20732.6	1.597	8.778	0.987	1	1.832
	4	0.945	0.042	4.074	0.998	45943.8	2.319	7.105	0.986	1	13.53
	6	0.982	0.024	3.204	0.937	11954.3	0.167	3.734	0.903	1.67	0.403
	7	0.968	0.018	2.853	0.947	22693.4	0.250	3.319	0.927	2	0.916
	8	0.991	0.030	4.123	0.963	13598	0.333	4.951	0.916	1.25	1.881
	10	0.946	0.035	3.965	0.997	42040.3	1.996	6.890	0.997	1.11	29.66

* Correlation is significant at 0.01 level (2-tailed).

tion rate expression is necessary in order to design a fast and effective process [35]. From a system design point of view, the analysis of bioadsorption rates using different kinetic equations is very important for practical operations [36–38]. Bioadsorption is a physiochemical process that involves the mass transfer of a solute (adsorbate) from the fluid phase to the bioadsorbent surface. In order to examine the mechanisms controlling the bioadsorption process, such as chemical reactions, intraparticular diffusion, and mass transfer through fluid films, several kinetic models are used to test the experimental data.

The kinetics of ^{67}Ga bioadsorption on FTW were analysed using pseudo-first-order, pseudo-second-order, and Elovich kinetic models. The best-fit model was selected based on the linear correlation coefficient, R^2, values. The rate equations are given in Table 5 and the related values in Table 6.

According to Table 6, the greatest correlation coefficient belongs to the pseudo-second order kinetic model; therefore, it can be concluded that the bioadsorption rate can be represented by this model. The Elovich kinetic model also well represented the kinetic data. This can indicate that chemisorption had an important role in this process because this model is in good agreement with the data of chemisorption processes [37].

3.11. Activation energy

The value of the activation energy from the Arhenius equation can also provide an indication whether a process is physical or chemical. The graph of $\ln k$ values of the pseudo-second-order rate constant (Table 6) versus $1/T$ yields the graph in Fig. 8.

$$\ln k = \ln A - \frac{E_a}{R}\frac{1}{T} \quad (20)$$

For the process, the activation energy of 23 kJ mol^{-1} is calculated from the slope of the line in Fig. 8. This high activation energy indicates that chemisorption plays an important contribution to the process [37]. Finally, considering all findings, it can be expressed that the bioadsorption process examined in this research is a result of physicochemical bioadsorption.

3.12. Bioadsorption mechanism

In a bioadsorption process, generally, three primary sequential steps occur—diffusion through the fluid layer around the particle, intra-particular or pore diffusion, and sorption on the surface. The Sorption on the surface is generally considered to be a very rapid process and its contribution to the resistance to mass transfer is usually negligible. The slower steps of film diffusion or pore diffusion or both can control the rate of the process. In the present research, the parameters which had considerable affects on bioadsorption were the initial pH of the solution and the bioadsorption dose. The effect of pH can be explained by the difference between the electrical charge of the adsorbed species and the surface charge; that is, the electrical force. The important effect of the particle size shows that the diffusion of ^{67}Ga through the pores in the bio-sorbent may be an important step in controlling the rate of the bio-sorption process. The small effect of the stirring speed is an indication that the diffusion through the film layer around the bio-sorbent particle was not a controlling step. Therefore, the process may not be controlled specifically by only one of the mechanisms diffusion through the film layer, surface sorption, or diffusion through the pores. The fact that the stirring speed did not have

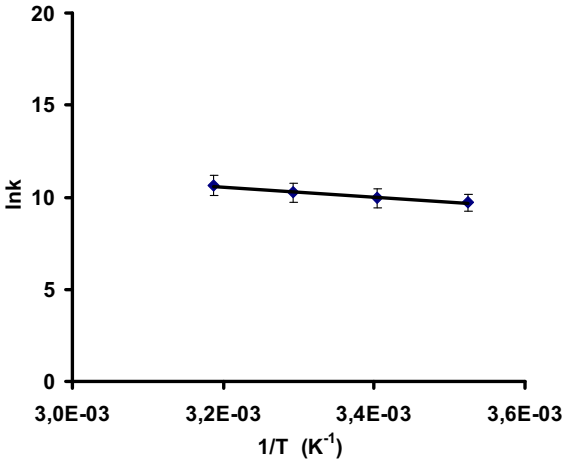

Fig. 8. Plot of $\ln k$ versus $1/T$.

Table 7
The calculations of intraparticle model.

Parameters		$t_{1/2}$	$k \times 10^9$	$D \times 10^{10}$	R^2
Temp. (°C)	10	7.9	9	5.19	0.982*
	20	5.5	9	7.45	0.919*
	30	4.2	8	9.75	0.847*
	40	2.9	6	14.12	0.866*
pH	2	5.5	9	5.19	0.919*
	4	3.1	6	13.21	0.810*
	6	22.4	4	1.83	0.991*
	7	13.3	4	3.08	0.985*
	8	14.9	6	2.75	0.982*
	10	3.5	6	11.70	0.879*

* Correlation is significant at the 0.01 level (2-tailed).

a significant affect on the process, and that the particle size has an important affect can be an indication that the process rate was controlled by pore/intraparticular diffusion [36–40].

If the intraparticular diffusion controls the process, the adsorbed amount (q_t) is a function of the square root of the adsorption period [36–40].

$$q_t = k_i\sqrt{t} + z \tag{21}$$

The value of the diffussion coefficient can be calculated by Eq. (22) [41–42].

$$f\left(\frac{q_t}{q_e}\right) = -\log\left[1 - \left(\frac{q_t}{q_e}\right)^2\right] = \frac{\pi^2 Dt}{2.3r^2} \tag{22}$$

If the rate process is considered to be pseudo-second-order, then;

$$t_{1/2} = \frac{1}{k.q_e} \tag{23}$$

The half-time can be expressed as:

$$D = \frac{0.030r^2}{t_{1/2}} \tag{24}$$

Table 7 shows the excellent agreement between the experimental and the calculated values. Therefore, it can be concluded that the controlling step is the diffusion through the pores in the particle. The increase of the diffusion coefficient with increasing temperature is an expected behaviour. However, the change of the diffusion coefficient with pH exhibited a complex behaviour because the Ga speciation changes with pH, and therefore, every species can have a different diffusion value. This effect can be explained by considering that Gallium ions become free of the citrate and hydroxyl ions with decreasing pH which causes the gallium ions to move more easily in the medium.

4. Conclusions

In this research, tea factory waste was used as an bioadsorbent to remove Ga, a radionuclide, from aqueous media. The process reached equilibrium in 120 min. The most effective parameters were determined to be, in decreasing order, pH, temperature, bioadsorbent nominal particle size, bioadsorbent dose, and stirring speed. The best bioadsorption conditions for the ranges of the parameters employed in the present research conducted at pH 2 were determined to be 600 rpm for the stirring speed, 0.150–0.212 mm for the nominal particle size, 20 °C for the temperature, and 10 g/L for the solid-to-liquid ratio. Under these conditions, 77.4% of the gallium was removed. The bioadsorption process exhibited an endothermic and multilayered character, and occurred physicochemically, which was confirmed by FTIR analysis. It was determined that the bioadsorption kinetics fitted well to the pseudo-second-order rate model, and that the bioadsorption process was controlled by intraparticular diffusion.

As a result, the bioadsorption by FTW can be a chip, fast and effective method for the removal of Ga-67. This is important because the Ga-67 itself and its stable daughter component Zn are potential posionous materials. The amount of Ga-67 in 1000 kg aqueous waste can be bioadsorbed on about 15 kg FTW. This simplifies the storage and handling of the radionuclides.

Acknowledgement

The support of Atatürk University for the project BAP-2003/372 is highly appreciated.

References

[1] H. Eroglu, Adsorption of radioactive thallium-201 and gallium-67 used in nuclear medicine, Ph.D. Thesis in Graduate School of Natural and Applied Sciences, Department of Environmental Engineering, Ataturk University, Turkey, 2009.
[2] R.J. Kowalsky, J.R. Perry, Radiopharmaceuticals in Nuclear Medicine Practice, Appleton & Lange, California, 1987.
[3] T.C. Basbakanlık, Özel işlem gerektirmeyen radyoaktif atiklara ilişkin yönetmelik, Resmi Gaz. 25771 (2004) 2–8.
[4] J.G. Dean, F.L. Bosqui, K.H. Lanoutte, Removing heavy metals from waste waters, Environ. Sci. Technol. 6 (1972) 518–524.
[5] J.C.P. Vaghetti, E.C. Limaa, B. Royer, J.L. Brasil, B.M. da Cunhaa, N.M. Simona, N.F. Cardoso, C.P.Z. Norenab, Application of Brazilian-pine fruit coat as a biosorbent to removal of Cr(VI) from aqueous solution—kinetics and equilibrium study, Biochem. Eng. J. 42 (2008) 67–76.
[6] B. Volesky, Bio-sorption and Bio-sorbents. Bio-sorption of Heavy Metals, CRP Press, Boca Raton, FL, 1990.
[7] E. Luef, P. Thedor, P.K. Christian, Adsorbtion of zinc by fungal mycelial wastes, Appl. Microbiol. Biotechnol. 34 (1991) 688–692.
[8] R.J.C. McLean, A.M. Campbell, P.T. Khu, A.T. Persaud, L.E. Bickerton, D. Chemin, Repea ted use of *Bacillus subtilis* cell walls for copper binding, J. Microbiol. Biotechnol. 10 (1994) 472–474.
[9] B. Volesky, Z.R. Holan, Adsorbtion of heavy metals, Biotechnol. Progr. 11 (1995) 235–250.
[10] B. Volesky, H.A. May-Philips, Adsorbtion of heavy metals by *Saccharomyces cerevisiae*, Appl. Microbiol. Biotechnol. 42 (1995) 797–806.
[11] E.İ. Medine, Adsorption of I-131 in urine of patent with amberlite anion exchange resin, M.Sc. in Nuclear Sciences Institute, Ege University, Turkey, 2003.
[12] H. Koshima, Adsorption of iron(III), gold(III), gallium(III), thallium(III) and antimony(V) on amberlite XAD and chelex 100 resins from hydrochloric acid solution, Anal. Sci. 2 (1986) 225–260.
[13] A.E. Osmanlioglu, Treatment of radioactive liquid waste by sorption on natural zeolite in Turkey, J. Hazard. Mater. B137 (2006) 332–335.
[14] C. Kütahyalı, Investigation of the selective uranium adsorption on activated carbon prepared from charcoal and its applications, Ph.D. Thesis in Nuclear Sciences, Ege University, Turkey, 2002.
[15] P.K. Sinha, K.B. Lal, J. Ahmed, Removal of radioiodine from liquid effluents, Waste Manag. 17 (1997) 33–37.
[16] A. Mudun, Meme kanserinde intraoperatif gama prob kullanımında radyasyon güvenliği, J. Breast Health 5 (2009) 115–118.
[17] A. Pekşen, A. Günay, Use of substrates prepared by the mixture of tea waste and wheat straw in *Agaricus bisporus* (L.) Sing. cultivation, Ekoloji 73 (2009) 48–54.
[18] H. Eroğlu, S. Yapıcı, Ç. Nuhoğlu, E. Varoğlu, An environmentally friendly process; adsorption of radionuclide Tl-201 on fibrous waste tea, J. Hazard. Mater. 163 (2009) 607–617.
[19] E.G. Jackson, M.J. Byrne, Metal ıon speciation in blood plasma: gallium-67-citrate and MRJ contrast agents, J. Nucl. Med. 37 (1996) 379–386.
[20] C.R. Bansal, M. Goyal, Adsorbtion Energetics, Model and Isotherm Equations. Activated Carbon Adsorbtion, Taylor and Francis Group, United States of America, 2005.
[21] H.Y. Erbil, Solid surfaces, B.E.T. multi-layer adsorbtion isotherm, in: Surface Chemistry of Solid and Liquid Interfaces, Blackwell Publishing, Gebze Institute of Technology, Turkey, 2006.
[22] J.D. Seader, E.J. Henley, Seperation Process Principles, John Wiley&Sons, Inc., Unided States of America, 1988.
[23] R.R. Bansode, J.N. Losso, W.E. Marshall, R.M. Rao, R.J. Portier, Adsorbtion of metals ions by pecan shell-based granual actived carbons, Bioresour. Technol. 89 (2003) 115–119.
[24] H.M. Jnr, A.I. Spiff, Equilibrium sorption study Of Al^{+3}, Co^{+2} and Ag^{+} in aqueous solutions by fluted pumpkin (Telfairia occidentalis HOOK f) waste biomass, Acta Chim. Slov. 52 (2005) 174–181.
[25] A.S. Luna, A.C.A. Da Costa, C.A. Henriques, M.H. Herbst, Electron paramagnetic resonance and atomic absorption spectrometry as tools for the investigation of Cu(II) biosorption by *Sargassum filipendula*, Hydrometallurgy 86 (2007) 105–113.

[26] S. Debnath, U.C. Ghosh, Kinetics, isotherm and thermodynamics for Cr(III) and Cr(VI) adsorption from aqueous solutions by crystalline hydrous titanium oxide, J. Chem. Thermodyn. 40 (2008) 67–77.
[27] I. Kiran, T. Akar, A.S. Ozcan, A. Ozcan, S. Tunali, Biosorption kinetics and isotherm studies of Acid Red 57 by dried *Cephalosporium aphidicola* cells from aqueous solutions, Biochem. Eng. J. 31 (2006) 197–203.
[28] S.S. Tahir, N. Rauf, Removal of a cationic dye from aqueous solutions by adsorbtion onto bentonite clay, Chemosphere 63 (2006) 1842–1848.
[29] S. Sun, A. Wang, Adsorption kinetics of Cu(II) ions using N,O-carboxymethylchitosan, J. Hazard. Mater. 131 (2006) 103–111.
[30] S.P. Dubey, K. Gopal, Application of natural adsorbent from silver impregnated *Arachis hypogaea* based thereon in the processes of hexavalent chromium for the purification of water, J. Hazard. Mater. 164 (2009) 968–975.
[31] W.J. Weber, J.C. Morris, J. Sanit, Kinetics of adsorbtion on carbon from solution, Eng. Div. 89 (1963) 31–59.
[32] G. Crini, H.N. Peindy, F. Gimbert, C. Robert, Removal of C.I. Basic Green 4 (Malachite Green) from aqueous solutions by adsorption using cyclodextrin-based adsorbent: kinetic and equilibrium studies, Sep. Purif. Technol. 53 (2007) 97–110.
[33] H. Lata, V.K. Garg, R.K. Gupta, Sequestration of nickel from aqueous solution onto activated carbon prepared from *Parthenium hysterophorus* L., J. Hazard. Mater. 157 (2008) 503–509.
[34] A. Baran, E. Bıçak, S.H. Baysal, S. Önal, Comparative studies on the adsorption of Cr(VI) ions on to various sorbents, Bioresour. Technol. 98 (2007) 661–665.
[35] M. Arami, N.Y. Limaee, N.M. Mahmoodia, Evaluation of the adsorption kinetics and equilibrium for the potential removal of acid dyes using a biosorbent, Chem. Eng. J. 139 (2008) 2–10.
[36] M. Alkan, M. Doğan, Y. Turhan, Ö. Demirbaş, P. Turan, Adsorption kinetics and mechanism of maxilon blue 5G dye on sepiolite from aqueous solutions, Chem. Eng. J. 139 (2008) 213–223.
[37] S.P. Silva, S. Sousa, J. Rodrigues, H. Antunes, J.J. Porter, I. Gonçalves, S.F. Dias, Adsorption of acid orange 7 dye in aqueous solutions by spent brewery grains, Sep. Purif. Technol. 40 (2004) 309–315.
[38] K. Biswas, S.K. Saha, U.C. Ghosh, Adsorption of fluoride from aqueous solution by a synthetic iron(III)–aluminum(III) mixed oxide, Ind. Eng. Chem. Res. 46 (2007) 5346–5356.
[39] Y.S. Ho, G. McKay, Sorption of dye from aqueous solution by peat, Chem. Eng. J. 70 (1998) 115–124.
[40] W.S.W. Ngah, M.A.K.M. Hanafiah, Adsorption of copper on rubber (*Hevea brasiliensis*) leaf powder: kinetic, equilibrium and thermodynamic studies, Biochem. Eng. J. 39 (2008) 521–530.
[41] A. Örnek, M. Özacar, İ.A. Şengil, Adsorption of lead onto formaldehyde or sulphuric acid treated acorn waste: equilibrium and kinetic studies, Biochem. Eng. J. 37 (2007) 192–200.
[42] B.E. Wang, Y.Y. Hu, L. Xie, K. Peng, Biosorbtion behavior of azo dye by inactive CMC immobilized *Aspergillus fumigatus beads*, Bioresour. Technol. 99 (2008) 794–800.